

1 *Technical Note*

2 **ASDToolkit: A Novel MATLAB Processing Toolbox** 3 **for ASD Field Spectroscopy Data**

4 **Kathryn Elmer¹, Raymond Soffer², J. Pablo Arroyo-Mora², and Margaret Kalacska^{1*}**

5 ¹ Applied Remote Sensing Lab, McGill University, Montreal, QC H3A-0B9, Canada

6 ² Flight Research Laboratory, National Research Council of Canada, Ottawa, ON, K1A-0R6, Canada

7 * Correspondence: margaret.kalacska@mcgill.ca

8 **Abstract:** Over the past 30 years, the use of field spectroscopy has risen in importance in remote
9 sensing studies for the characterization of the surface reflectance of materials *in situ* within a broad
10 range of applications. Potential uses range from measurements of individual targets of interest (e.g.
11 vegetation, soils, validation targets etc.), to characterizing the contributions of different materials
12 within larger spatially-mixed areas as would be representative of the spatial resolution captured by
13 a sensor pixel (UAV to satellite scale). As such, it is essential that a complete and rigorous assessment
14 of both the data-acquisition procedures, and the suitability of the derived data product be carried
15 out. The measured energy from solar-reflected range spectroradiometers is influenced by the
16 viewing and illumination geometries and the illumination conditions which vary due to changes in
17 solar position and atmospheric conditions. By applying corrections, the estimated absolute
18 reflectance (R_{abs}) of targets can be calculated. This property is independent of illumination intensity
19 or conditions and is the metric commonly suggested to be used to compare spectra even when data
20 are collected by different sensors or acquired under different conditions. By standardizing the
21 process of estimated R_{abs} , as is provided in the described toolkit, consistency and repeatability in
22 processing are ensured and the otherwise labor intensive and error-prone processing steps are
23 streamlined. The resultant end data product (R_{abs}) represents our best current effort to generate
24 consistent and comparable ground spectra which have been corrected for viewing and illumination
25 geometries as well as other factors such as the individual characteristics of the reference panel used
26 during acquisition.

27 **Dataset:** <http://doi.org/10.5281/zenodo.3996377>

28 **Dataset License:** GNU GPL 3.0

29 **Keywords:** spectral processing; reflectance; spectrometer; spectroradiometer
30

31 **1. Introduction**

32 Field spectroscopy has long played a key role in the collection of spectral information used for a
33 broad range of remote sensing studies [1-3]. Surface reflectance data have applications in multiple
34 disciplines such as forestry [4], agriculture [5], mining [6], calibration and validation [3, 9] and many
35 others. Solar-reflected spectroscopy data (i.e. near ultraviolet to shortwave infrared) from portable
36 field spectrometers contain detailed information regarding the physical properties and chemical
37 composition of materials. The measured reflected energy (in digital numbers or units of radiance) is
38 influenced by illumination conditions and can vary substantially over the course of a day due to
39 changes in solar position and/or atmospheric conditions. In Earth observation applications within
40 this spectral range, the fundamental property of interest is the spectral reflectance of a target or
41 material of interest. In its most basic form, it is the ratio of incident-to-reflected radiance over a set of
42 wavelengths (R_{ratio} , also referred to as the *relative reflectance*) and is a unique property of a given target
43 [7]. Many studies utilize the R_{ratio} as directly calculated by the instrument. However, doing so causes

44 substantial challenges in making valid comparisons of spectra of the same material over time, spectra
 45 acquired at different locations or by different instruments or reference targets. As described by [2],
 46 the generation of R_{ratio} requires a second surface, the reference panel, to be used as a bright
 47 (approaching 100% reflectance), theoretically Lambertian (i.e. diffuse) target with which the ratio is
 48 calculated. As such, the spectral and angular properties of the reference panel directly affect R_{ratio} .
 49 The *absolute spectral reflectance* of a material (R_{abs}), in contrast, is independent of illumination intensity
 50 or conditions. The suggested metric allowing comparison of spectra even if collected by different
 51 sensors, acquired under different conditions (e.g. time, location, orientation) [7], or with different
 52 reference panels is therefore R_{abs} .

53 In order to generate standardized, representative and comparable R_{abs} , there are multiple factors
 54 to consider, including the influence of downwelling irradiance from direct (e.g. the sun) and diffuse
 55 (e.g. the sky) sources on the target(s) of interest, and the spectral characteristics of the reference
 56 material (e.g. 99% reflective Spectralon®) against which the target is measured. In order to account
 57 for these factors, a primary component of the calculations is the computation of the hemispherical
 58 conical reflectance factor (HCRF) of the target of interest, which best describes the real-world
 59 illumination and viewing geometry encountered in field spectroscopy, and the property “measured”
 60 by spectroradiometers [2]. HCRF represents the ratio of downwelling direct and diffuse irradiance to
 61 reflected conical radiance (see Figure 3 Case 8 in [2] for a schematic representation). By applying
 62 corrections for variations in solar illumination conditions during the measurement period and the
 63 individual spectral characteristics of the reference panel used during acquisition, a more accurate
 64 approximation of the estimated R_{abs} can be achieved. ASDToolkit is a standalone application for
 65 generating estimated R_{abs} from the commonly acquired R_{ratio} provided by the ASD FieldSpec series of
 66 spectroradiometers (Malvern Panalytical Company, Longmont, CO, USA).

67 2. Description of ASDToolkit

68 2.1 Theoretical background

69 Central to the calculation of the estimated R_{abs} is the recognition that reference panels are neither
 70 perfectly Lambertian, nor is their reflectance uniform across the solar-reflected range [2]. These two
 71 aspects must be accounted for. Reflectance properties of materials with some degree of anisotropy
 72 result in their reflectance not being perfectly Lambertian; this directional characteristic of the
 73 reflectance when accounted for from all angles is the bidirectional reflectance-distribution function
 74 (BRDF) [8]. Importantly, BRDF is a theoretical property of materials which cannot be reliably
 75 measured in the field [2]. Instead, under normal field conditions it is the HCRF which is often
 76 measured, as shown in Equation 1,

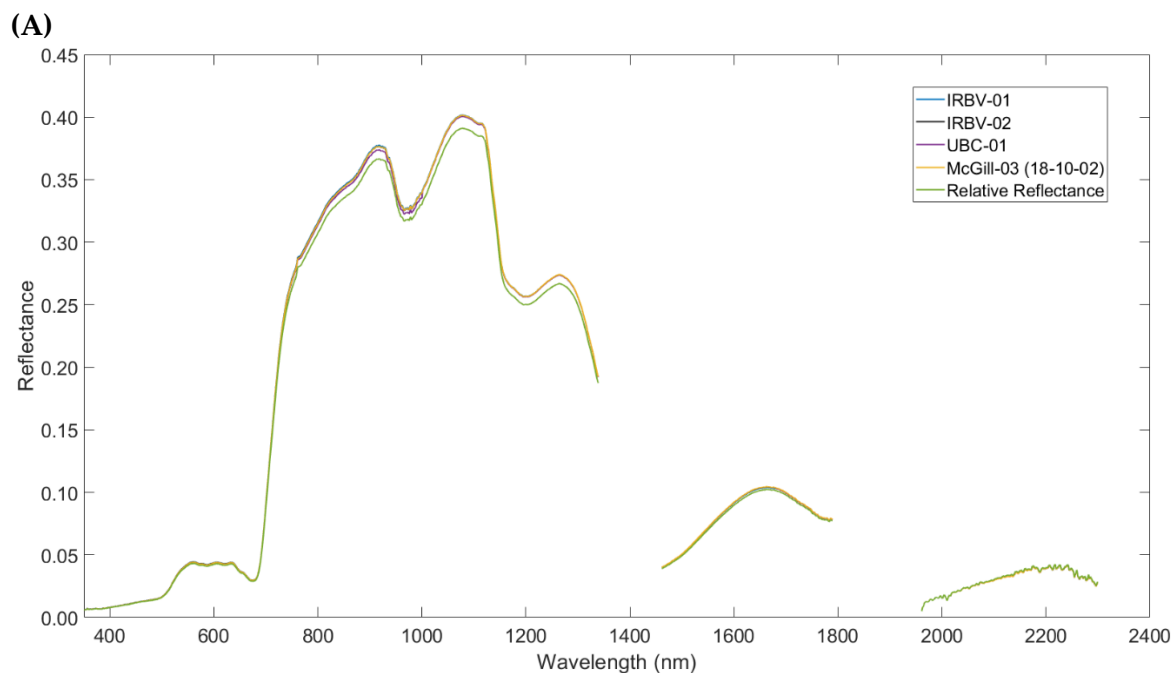
$$HCRF = \frac{S_{tar}}{S_{ref}} \times R_{ref} \quad (1)$$

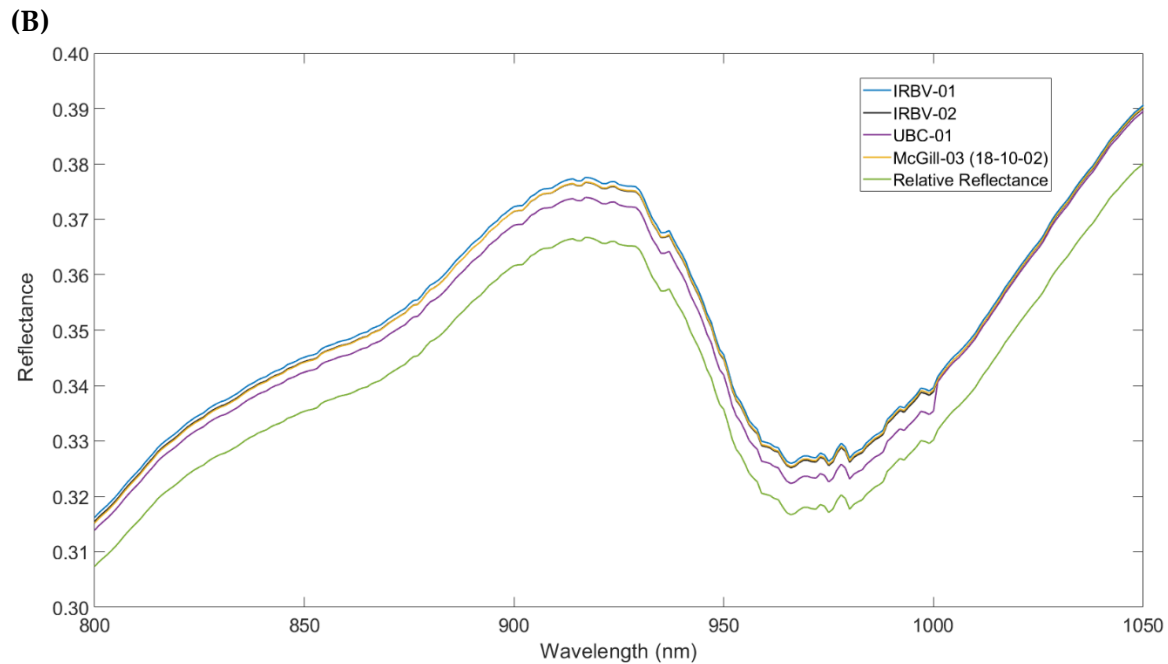
77 where S_{tar} is the signal of the target, S_{ref} is the signal of the reference panel, and R_{ref} is the
 78 reflectance of the reference panel. As mentioned previously, R_{ratio} erroneously assumes a Lambertian
 79 reference panel with a reflectance of 1.0 across wavelengths whereas Eq. 1 calculates the appropriate
 80 value for R_{ref} . The signal (S) does not need to be in units of radiance, but instead can be a value that
 81 is linearly proportional to radiance such as digital numbers (DN). The implication of this is that
 82 maintenance of the radiometric calibration of the field spectrometer is not essential as long as the
 83 system has a linear response and is stable [3,9].

84 While proper field acquisition protocols can mitigate some of the challenges posed by the
 85 spectral and angular properties of reference panels, this alone is not enough to generate reliable R_{abs} .
 86 The most common and best characterized material from which reference panels are made is
 87 Spectralon® [9]. Its spectral properties are well characterized [10] and it has a high reflectance
 88 throughout the solar-reflected region. Nevertheless, its reflectance does vary according to viewing
 89 and illumination geometries [10,11], wavelength of observation [12,13], and it is known to degrade

90 over time [14-17]. Spectralon® panels, when purchased with calibration from the manufacturer, are
91 provided with Conical-Hemispherical Reflectance Factor coefficients measured empirically in an
92 8°:hemispherical illumination:viewing geometry configuration (Figure 3 Case 6 in [2]). Multiplication
93 of these coefficients with the R_{ratio} provides a significant improvement over only using R_{ratio} by
94 introducing the relative spectral profile of the reference panel.

95 Taking these corrections a step further is to include compensation for the combined direct solar
96 irradiance and anisotropic diffuse sky downwelling irradiance encountered in the field by
97 application of a BiConical Reflectance Factor (BCRF) to the reference panel's CHRF. This applied
98 BCRF, determined in the laboratory (see [9] for details), is referred to as $BCRF(0^\circ:45^\circ)$ or the $R(0^\circ:45^\circ)$
99 reflectance factor of the panel (i.e. nadir view: 45° illumination). Due to the known angular
100 dependencies of the reflectance properties of Spectralon®, this $R(0^\circ:45^\circ)$ reflectance factor needs to be
101 adjusted to the observed illumination geometry (assuming a nadir viewing angle) caused by the solar
102 zenith angle (SZA) at the time and location of data acquisition. This normalized BCRF, or nBCRF, is
103 a function of the illumination angle and is wavelength independent [2,18]. The SZA adjusted nBCRF,
104 $nBCRF(SZA)$, is the specific value at the given illumination angle [10,18]. The nBCRF has been shown
105 to be consistent both as a function of wavelength and between new and lightly used 99% reflective
106 Spectralon® panels [9,10]. The $BCRF(0^\circ:SZA^\circ)$ can be derived by multiplying $BCRF(0^\circ:45^\circ)$ by
107 $nBCRF(SZA)$, and has been determined to be valid for 99% reflective Spectralon® reference panels
108 used in clear conditions under SZA from near nadir to 60° [18]. Ultimately, this reference panel
109 specific $BCRF(0^\circ:SZA^\circ)$ adjusted R_{ratio} is the estimated R_{abs} calculated by the toolkit. The significance
110 of these corrections is apparent in Figure 1 which illustrates a vegetation spectrum acquired under a
111 SZA of 42.25°, in which the direct illumination angle differs from the normalization geometry by
112 2.75°. Through the application of these calculations and adjustments to R_{ratio} a more accurate estimate
113 of the target's R_{abs} is achieved. Details regarding the physical basis for the concepts and the theoretical
114 methodology for the estimation of R_{abs} can be found in [7] and [9].
115





116 Figure 1. Example of estimated R_{abs} calculated by the toolkit. Spectra are of vegetation acquired under a
 117 SZA of 42.25° . It is important to note that the difference between R_{ratio} (relative reflectance) and estimated
 118 R_{abs} will vary as a function of the SZA. A) comparison of R_{ratio} and R_{abs} as estimated using the BCRF($0^\circ:45^\circ$)
 119 of four different 99% Spectralon[®] panels of various ages: McGill-03, IRBV-01, IRBV-02, and UBC-01. The
 120 actual panel used in the field during data acquisition of this spectrum was McGill-03 making this the best
 121 estimate of R_{abs} . B) An enlargement of spectrum from A over the 800-1050 nm range illustrating the impact
 122 of calculating estimated R_{abs} from R_{ratio} using different panels.

123 2.2 Overview of the ASD FieldSpec 3 and Data Acquisition

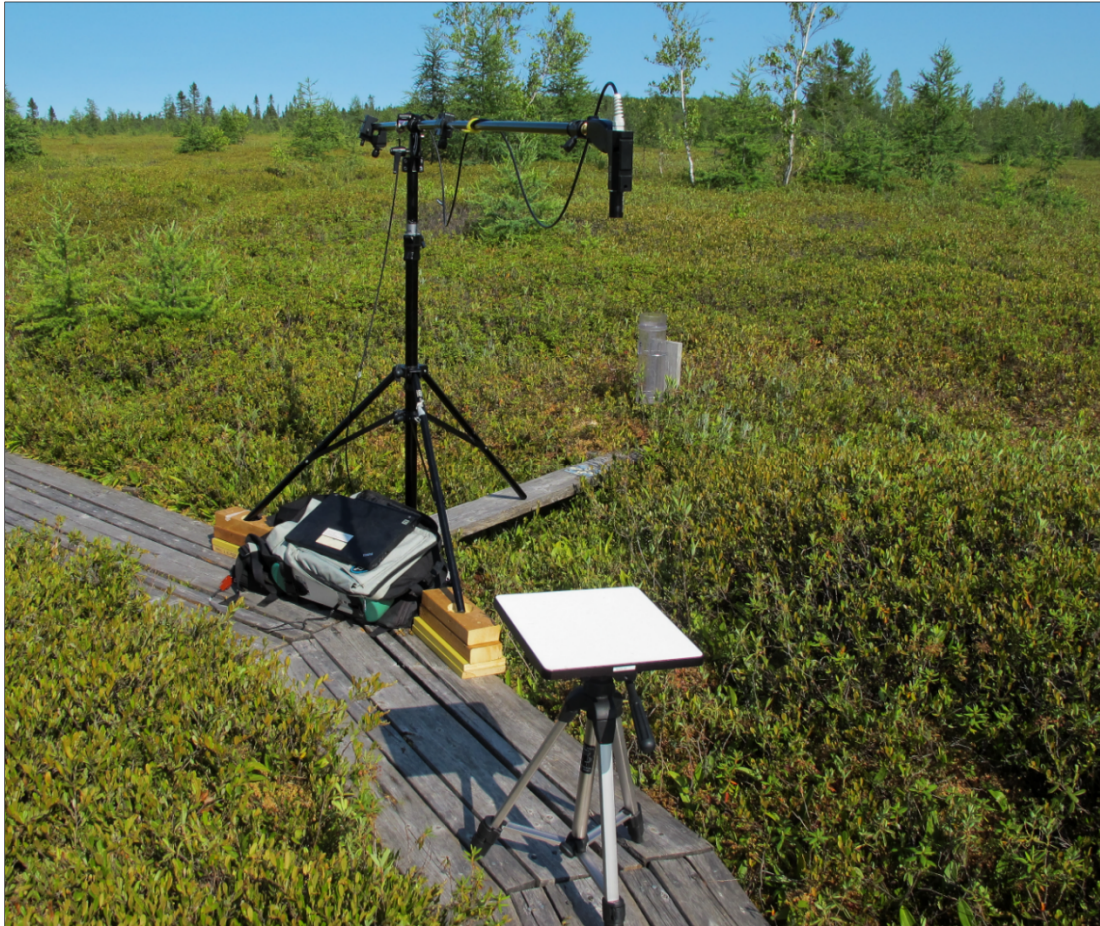
124 Even though the ASDToolkit was developed for calculation of R_{abs} from ASD FieldSpec 3 data,
 125 it is not dependent on this specific model of instrument and is therefore compatible with spectra
 126 collected using other models as well. The ASD FieldSpec 3 is comprised of three separate internal
 127 spectrometers covering a spectral range of 350-2500 nm across the near UV to SWIR regions. Details
 128 about the instrument are given in Table 1, as well as in the ASD FieldSpec 3 user manual [19].

129 **Table 1.** Primary specifications of the ASD FieldSpec 3. FWHM refers to the Full-Width-Half-
 130 Maximum

| Characteristic | Range |
|-----------------------|---|
| Spectral range | VNIR: 350 – 1050 nm SWIR1: 1000 – 1800 nm SWIR2: 1800 – 2500 nm |
| Spectral resolution | 3 nm FWHM at 700 nm 10 nm FWHM at 1400 & 2100 nm |
| Sampling interval | 1.4 nm at 350 – 1050 nm 2 nm at 1000 – 2500 nm |
| No. of optical fibers | VNIR: 19 fibers (100 μm) SWIR1-2: 38 fibers (200 μm) |

131 Collection of in situ field spectra using the ASD FieldSpec 3 should follow a routine and
132 standardized procedure (see [20] for an example protocol). The instrument set up in the field is
133 shown in Figure 2.

134



135

136 Figure 2. An example of the ASD FieldSpec 3 instrument setup in the field for data acquisition using
137 a tripod, the fiber optic cable extension, pistol grip, and a 99% Spectralon panel as white reference.

138 2.3. Overview of ASDToolkit

139 ASDToolkit was created in MATLAB® and consists of a single-window user interface. The toolkit
140 does not require any coding knowledge or coding inputs from the user. It is currently available for a
141 Microsoft Windows operating system. ASDToolkit is launched from the executable file and requires
142 MATLAB® Runtime to be installed. The MATLAB® Runtime installer and instructions are included
143 with the ASDToolkit download package. The fundamental spectroscopy concepts that provide the
144 basis for the processing methodology used by ASDToolkit are discussed at length in [7] and [9]. These
145 concepts were refined in order to translate effectively into a MATLAB-based processing interface.

146 2.4. Preparation of ASD Data Files

147 The input format requires ASCII files in which the dark current corrected signals in DN
148 have been processed to R_{ratio} . The ASCII file is expected to contain the standard ASD acquisition
149 header information followed by a single spectrum organized as two tab delimited columns with the
150 first column containing the wavelength and the second the value of R_{ratio} (Figure 3). A straightforward
151 way to generate these input files is through the freely available software ViewSpecPro which can be
152 downloaded from Malvern Panalytical [21]. If using ViewSpecPro to generate the input files, they
153 need to be processed using the “ASCII export” option with “Reflectance” selected as the output data

154 format. A detailed user guide on how to correctly pre-process the ASD data files in ViewSpecPro is
 155 included with the documentation bundled with the ASDToolkit [22].
 156

```

The instrument number was 16478/1
New ASD spectrum file: Program version = 6.00 file version = 7.00
Spectrum saved: 10/26/2019 at 23:19:58
VNIR integration time : 34
VNIR channel 1 wavelength = 350 wavelength step = 1
There were 25 samples per data value
xmin = 350 xmax= 2500
ymin= 0 ymax= 1.25
The instrument digitizes spectral values to 16 bits
SWIR1 gain was 444 offset was 2147
SWIR2 gain was 822 offset was 2312
Join between VNIR and SWIR1 was 1000 nm
Join between SWIR1 and SWIR2 was 1830 nm
VNIR dark signal subtracted
25 dark measurements taken Sat Oct 26 23:19:08 2019
DCC value was 0
Data is compared to a white reference:
25 white reference measurements taken Sat Oct 26 23:19:11 2019
There was no foreoptic attached
Spectrum file is raw data with embedded reference
GPS-Latitude is S0
GPS-Longitude is E0
GPS-Altitude is 0
GPS-UTC is 00:00:00

Smart Detector
Serial# 0
Signal (A) 0.000E00
Dark (A) 0.000E00
Ref (A) 0.000E00
Status 0 - Uninitialized
Gain E-4
Averaging 0
Temp (C) 0.0
Humid (%) 0.0

Wavelength      acnodon_aoc00000.asd
350      0.111667590595262
351      0.113446348842323
352      0.119572560669084
353      0.126693052836344
354      0.135916942165335
355      0.12907505681874
356      0.120939977534611
357      0.126698367262935
358      0.123256503742685
359      0.12275596098911
360      0.12581454930843
  
```

157
 158 Figure 3. Example of the expected format of an ASCII file for input to the toolkit. Only wavelengths
 159 350 – 360 nm are shown. This file of R_{ratio} was generated in ViewSpecPro.

160 2.5 Required User Files

161 The necessary input files include the R_{ratio} data files (as described in section 2.4), as well as
 162 reference panel characteristic files. Panel characteristic files are ASCII files containing the
 163 BCRF($0^{\circ}:45^{\circ}$) information of the reference panel used to acquire the spectra in the field. The
 164 ASDToolkit includes several predefined panels that have been characterized under laboratory
 165 conditions by the National Research Council of Canada (NRC) Flight Research Laboratory using the
 166 methodology described in [9]. Users have the option of supplying their own panel characteristic file
 167 for any panel(s) used in their data collection activities or to capture degradation in the panel
 168 reflectance factors that typically occurs over time with use in the field. This is recommended to ensure
 169 accuracy of the results. The format of the user-defined panel characteristic file is specific and requires
 170 the following:

- 171 1) the file must be a .csv
- 172 2) the first row in the first column must contain a panel identifier or panel characteristic file name
- 173 3) the wavelengths must only be in the first column, beginning at row two
- 174 4) the panel measurement data must only be in the second column, beginning at row two
- 175 5) the panel measurements must be provided at the same wavelength intervals as the R_{ratio} files.

176 Incorrect formatting will lead to incorrect processing of the data files. An example panel characteristic
 177 file is shown in Figure 4 and is provided in the toolkit download package.

| Wavelength (nm) | Ratio |
|-----------------|--------|
| 350 | 1.0086 |
| 351 | 1.0085 |
| 352 | 1.0085 |
| 353 | 1.0085 |
| 354 | 1.0085 |
| 355 | 1.0085 |
| 356 | 1.0084 |
| 357 | 1.0084 |
| 358 | 1.0084 |
| 359 | 1.0084 |
| 360 | 1.0084 |
| 361 | 1.0084 |
| 362 | 1.0084 |
| 363 | 1.0084 |
| 364 | 1.0084 |
| 365 | 1.0084 |
| 366 | 1.0084 |
| 367 | 1.0084 |
| 368 | 1.0084 |
| 369 | 1.0084 |
| 370 | 1.0084 |
| 371 | 1.0085 |
| 372 | 1.0085 |
| 373 | 1.0085 |
| 374 | 1.0085 |
| 375 | 1.0085 |
| 376 | 1.0086 |
| 377 | 1.0086 |
| 378 | 1.0086 |

178

179

180

Figure 4. Example of the expected format of a panel characteristic file. Only wavelengths 350 – 378 nm are shown.

181

182

183

184

185

186

187

188

189

The R_{ratio} files should be contained in a single folder by common latitude/longitude/elevation, as the ASDToolkit assumes a constant location for processing all files contained within the input folder. Changes in latitude/longitude greater than one arc-minute or 0.016667 decimal degrees (~1.83 km of linear distance in latitude but varies in longitude) will result in differences in the calculated values for the solar angles having a noticeable impact on the final result. Therefore, this sensitivity to location means that spectra collected within approximately 1 arc-minute range can be processed together. Spectra collected outside this range should be processed separately to ensure correct solar angle calculations.

190

2.6 Description of User Inputs to the ASDToolkit Interface

191

192

193

194

195

196

197

198

The ASDToolkit user interface (Figure 5) consists of a graphical user interface (GUI) with one main window where the user selects the inputs and processing options. Inputs may be supplied to the appropriate fields in any order, however, all input fields are required. Upon launching the ASDToolkit executable, the user is presented with the main interface window. There are several options for processing R_{ratio} files, including multiple selection choices for the reference panel to use, an option to apply an Incident Angle Correction Factor (IACF) to account for a time offset between collection of the reference measurement and target measurements (calculated from the embedded time stamp and provided location coordinates), an option to apply a spectral discontinuity correction

199 at the cross-over wavelengths between the three spectrometers (i.e. 1000 and 1800 nm), and options
 200 to override the illumination conditions using two common lab-based illumination and viewing
 201 geometries. These options and necessary inputs are described in detail below.

202

203

Figure 5. Main interface window where the user selects the inputs and processing options.

204

205

206

207

208

209

210

211

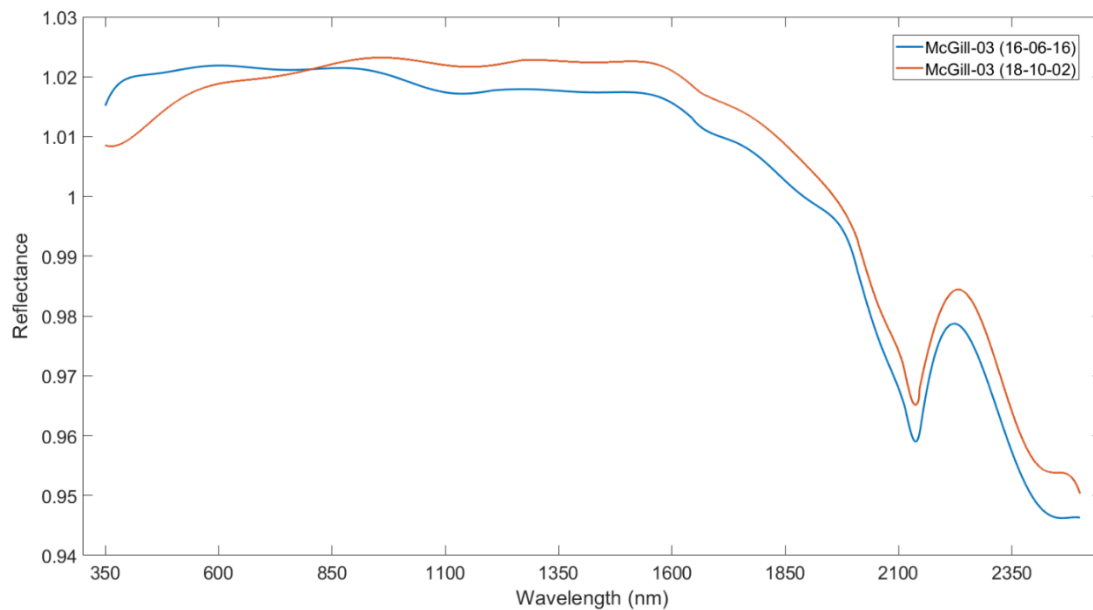
212

213

214

215

In the “Select Reference Panel” window, the user selects the reference panel to be used for processing. Several panels are included, with the date of calibration given in parentheses appended to the panel name in the list window. Multiple calibrations for a given panel are important if the same panel is used over long periods of times (e.g. years) or suffers excessive degradation due to use. As an example, the two calibrations of the McGill-03 99% Spectralon® panel are shown in Figure 6. To use a reference panel not supplied in the default list, a custom user provided panel characteristic file must be supplied (as described in Section 2.5). To enable a custom panel, the user should select the “User Supplied” option from the list window. The “>>” button next to the panel list selection is used to set the working directory for the ASDToolkit. It is necessary to leave the working directory as the default path where the ASDToolkit executable is located. Failure to do so will result in the inability of the toolkit to process the files.



216

217 Figure 6. Degradation of the McGill-03 99% reflective Spectralon® panel between two calibration
 218 dates (June 16, 2016 and October 02, 2018).

219 The user is required to enter the latitude and longitude (in decimal degrees), as well as elevation
 220 (in km above sea level) at which the spectra were acquired. Elevation data is collected for metadata
 221 purposes only and is not used in any calculations. For latitude and longitude, North and East are
 222 positive (sign not required) and South and West are negative (sign required). The equations and
 223 constants to calculate the solar angles are implemented from [7] and [23] and verified for accuracy
 224 against results from [24]. As solar angles are calculated using astronomical algorithms, they do not
 225 require a specific horizontal or vertical datum. The number of hours offset from Universal Time
 226 Coordinated (UTC) based on the time zone applied to the embedded time stamp must also be entered.
 227 For example, Eastern Standard Time has an offset of -4 hours from UTC during the months of March
 228 to November (accounting for daylight standard time) and an offset of -5 hours from UTC during
 229 December to February. Using the entered offset, the toolkit converts the collection time found in the
 230 R_{ratio} file headers to UTC for processing.

231 The ASDToolkit provides the option to override the illumination (i.e. elevation and
 232 azimuth) calculated using solar angle geometry based on the latitude/longitude at which the spectra
 233 were acquired. Overriding the illumination calculation sets the viewing:illumination geometry to
 234 0°:45°, or 0°:23°, the standard time independent geometries encountered in a laboratory setting and
 235 when acquiring spectra with the ASD contact probe accessory. For data collected in the field under
 236 natural solar illumination conditions, this override option should be set to “None” so that the
 237 illumination geometry is calculated.

238 Another processing option is whether an Incident Angle Correction Factor (IACF) [9] is
 239 applied to account for systematic variances in the downwelling irradiance conditions due to
 240 progression in the solar geometry between the acquisition times of the reference panel and target
 241 measurement. If the reference measurement and target measurement are acquired close together in
 242 time, the effect of the IACF will be minimal. However, if enough time has elapsed between collection
 243 of the reference measurement and target measurement(s), the IACF calculates a correction factor by
 244 taking the cosine of the solar zenith angle for the reference measurement divided by the cosine of the
 245 solar zenith angle for the target measurement. Benefits of this correction under natural solar
 246 illumination conditions have been shown to be evident for periods of time as short as 5 minutes (see
 247 Figure 12 of [9]). The IACF is calculated using Equation 2:

248

$$249 \quad IACF = \frac{\cos(SZA_{reference})}{\cos(SZA_{target})} \quad (2)$$

250 where $SZA_{reference}$ is the calculated solar zenith angle (degrees) at the time that the reference
251 measurement was collected, and SZA_{target} is the calculated solar zenith angle (degrees) at the time
252 that the target measurement was collected. Once the IACF has been calculated, it is then used to scale
253 the associated spectral reflectance values for each individual file prior to application. The ASDToolkit
254 provides output files containing both the estimated R_{abs} and the estimated R_{abs} with the IACF applied
255 for user comparison. Additionally, a column containing the individual IACF values for each
256 processed file's individual timestamp is included in the output MATLAB® structure.

257 The ASD FieldSpec spectrometers have known spectral discontinuities originating from
258 multiple potential sources [19,25-27] and may result in spectral "steps" in the reflectance values at
259 the wavelength thresholds between the three internal spectrometers, namely 1000 nm and 1800 nm.
260 Certain conditions may cause these discontinuities to become more or less pronounced. The VNIR
261 fiber bundle has a slightly broader FOV than those of the two SWIR instruments (see Figure 4 in [27]).
262 Therefore, one of the most common causes for the discontinuities in the reflectance is due to shading
263 differences between the VNIR and SWIR data leading to differences in the radiance measured by
264 each detector [19]. Excessive discontinuities are due to other factors such as use of the instrument
265 prior to achieving thermal stability following power on which can be of significant duration (an hour
266 or longer) under extreme and rapid temperature changes. Use of a lens to reduce the FOV with
267 heterogeneous or specular targets can also result in exaggerated discontinuities. ViewSpecPro
268 contains an option for a "parabolic correction" to mitigate these discontinuities [19]. If it is not applied
269 a processing option is included in this toolkit to apply a "discontinuity correction" to the data [28]. It
270 is important to note that the calculation of the discontinuity correction solutions performed by the
271 toolkit is based on estimating the gradient between the edges of the discontinuity and calculating an
272 additive and multiplicative solution to blend the two edges of the discontinuity together, rather than
273 calculate a solution based on a specific empirical model. If the discontinuity correction option is
274 selected, these solutions are provided in additional files separate from the original processed spectra
275 so that the user can evaluate the results

276 Lastly, the user must select the input directory, which is the folder that contains the R_{ratio}
277 files (pre-processed as per section 2.4). The selected output directory is where all of the generated
278 results files will be saved. Both the input and output file directories may be selected by clicking the
279 associated "Browse" button or the full path name can be entered into the user input box. The output
280 variable name is the root file name that all the processed files will share, with additional file naming
281 conventions appended automatically such as *"*_estimatedAbsoluteReflectance"*, *"*_headerInfo"*,
282 *"*_estimatedAbsoluteReflectance_IACF"* and others (see section 3.2).

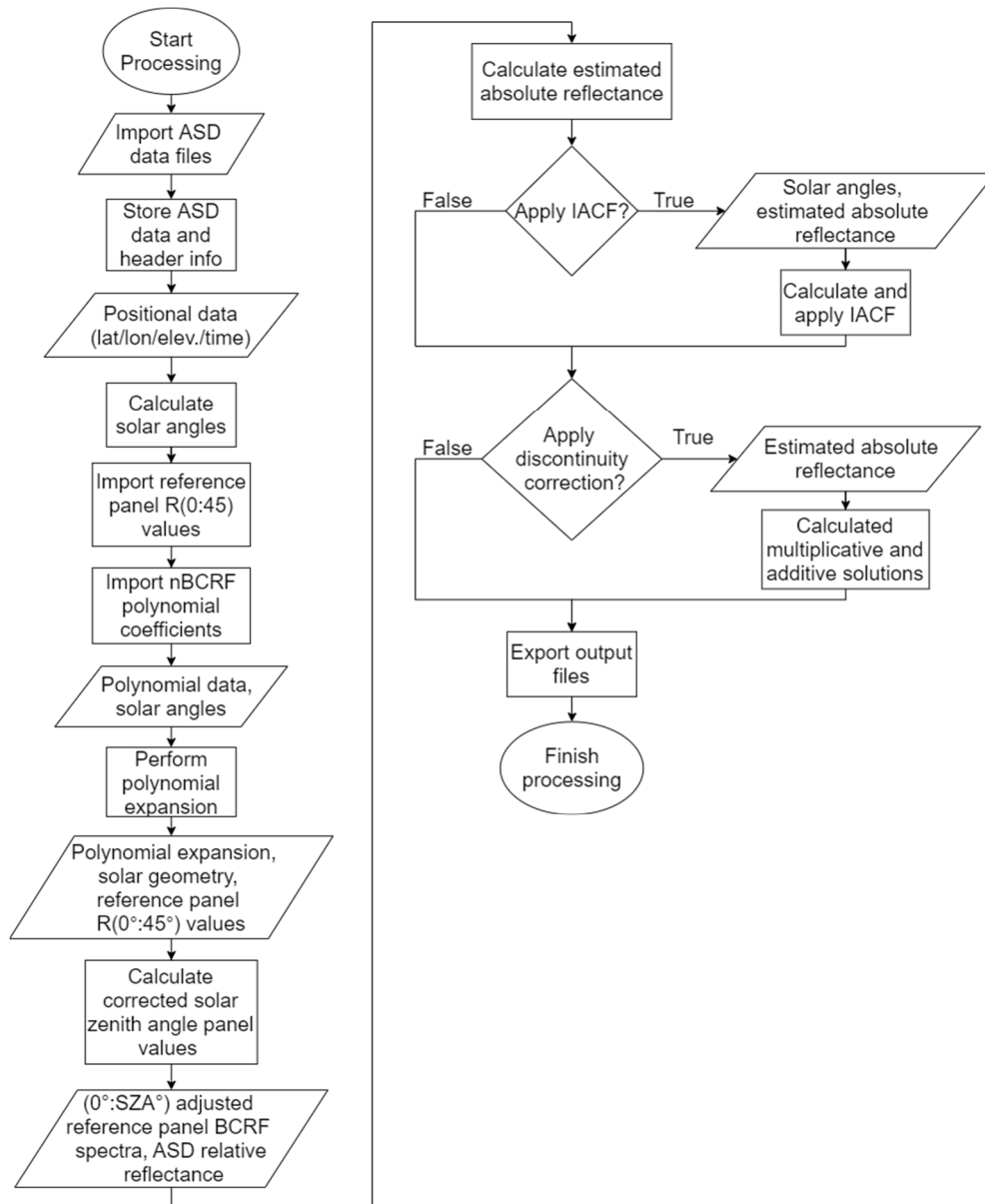
283 Once the user has entered the required inputs, the toolkit can then be executed. If there are
284 any errors in the inputs, such as improper latitude/longitude data, blank fields, invalid file types or
285 invalid directories, then specific error messages will appear that detail which error occurred and the
286 changes required to the inputs to resolve the error. The user can close the error message window and
287 fix the erroneous inputs as necessary and proceed to run the toolkit again without needing to
288 completely re-enter all the other inputs. If the user selected the "User Supplied" option in the panel
289 list, then a new window will open prompting the user to navigate to the correct directory and select
290 the custom user defined panel characteristic file. If one of the pre-defined panels is selected, the toolkit
291 will begin to process the selected data files immediately and a progress bar will appear during
292 processing. Once the processing is complete, a message will be displayed on the screen that indicates
293 the processing has been completed successfully. The user may then navigate away from the
294 ASDToolkit interface (either minimizing or completely closing the interface window) to the output
295 directory and locate the output files. A video walk-through of the ASDToolkit is shown in
296 Supplementary Video 1.

297
298

299 3. Methodology

300 3.1 ASDToolkit Workflow

301 The internal processing workflow is shown in detail in Figure 7 and described below.
302 1. Import Necessary Reflectance Files [29]
303 • Inputs: ASD data files
304 • Outputs: ASD relative reflectance data, header information (time, date, wavelength, etc.)
305 2. Calculate the Solar Zenith Angles
306 • Inputs: ASD data file header information (date, time), latitude/longitude information, hours
307 offset from UTC
308 • Outputs: Solar Azimuth Angle, Solar Zenith Angle
309 3. Import Panel Specific Values for $R(0^\circ:45^\circ)$
310 • Inputs: Reference panel characteristic files (pre-defined or user supplied)
311 • Outputs: Panel characteristic information
312 4. Import nBCRF Polynomial Coefficients
313 • Inputs: Panel independent BCRF ($0^\circ:45^\circ$)
314 • Outputs: nBCRF polynomial parameters
315 5. Polynomial Expansion
316 • Inputs: Panel specific BCRF ($0^\circ:45^\circ$), solar geometry data, nBCRF polynomial parameters
317 • Outputs: polynomial expansion results adjusted for normalized BCRF
318 6. Calculate the Corrected Solar Zenith Angle Panel Values
319 • Inputs: Average polynomial expansion results, solar geometry data
320 • Outputs: ($0^\circ:SZA^\circ$) adjusted reference panel BCRF spectra for the given panel
321 7. Calculate Estimated Absolute Reflectance
322 • Inputs: SZA adjusted panel BCRF, ASD relative reflectance data
323 • Outputs: Estimated absolute reflectance values
324 8. Apply IACF or Not
325 • Inputs: Solar Zenith Angle of reference measurement, Solar Zenith Angle of target
326 measurement
327 • Outputs: Estimated absolute reflectance values with IACF applied
328 9. Apply Discontinuity Correction
329 • Inputs: Estimated absolute reflectance values
330 • Outputs: Estimated absolute reflectance values with correction applied
331 10. Export Results
332 • Inputs: Estimated absolute reflectance data structure
333 • Outputs: Header file, estimated absolute reflectance data structure (as a MATLAB file and
334 an Excel file), IACF file, Discontinuity correction files (additive and multiplicative solutions)
335
336



337

338

Figure 7. Flowchart of the internal processing workflow of the toolkit.

339 3.2 ASDToolkit Output Files

340 Depending on the processing options selected in the interface window, optional output files may
 341 be generated. Files that are always generated are:

- 342 • *variablename.mat*: a MATLAB® (*.mat) data file that contains all of the processed data and header
 343 information and can be opened directly in MATLAB® for further data manipulation.
- 344 • *variablename_estimatedAbsoluteReflectance.csv*: A (*.csv) file that contains the estimated absolute
 345 reflectance output values where each column represents a single data file, with the name of the
 346 file as the first row in each column.
- 347 • *variablename_headerInfo.csv*: A (*.csv) file that contains the detailed header information for each
 348 processed file, where each column represents a single data file that was processed.

349

350 Optional files that are generated based the selected processing options are:

- 351 • *variablename_estimatedAbsoluteReflectance_IACF.csv*: Generated when the IACF option is selected
 352 in the interface. A (*.csv) file that contains the estimated absolute reflectance output values with
 353 the IACF applied, where each column represents a single data file, with the name of the file as
 354 the first row in each column.

- 355 • *variablename_DC_additive.csv*: Generated when the Discontinuity Correction option is selected in
 356 the interface. A (*.csv) file that contains the estimated absolute reflectance values for the additive
 357 solution, where each column represents a single data file, with the name of the file as the first
 358 row in each column.
- 359 • *variablename_DC_multiplicative.csv*: Generated when the Discontinuity Correction option is
 360 selected in the interface. A (*.csv) file that contains the estimated absolute reflectance values for
 361 the multiplicative solution, where each column represents a single data file, with the name of
 362 the file as the first row in each column.

363 3.4 Details on the generated MATLAB® Data File (*.mat)

364 As described in section 3.3, one of the output files that is always generated is the MATLAB® data
 365 file (*.mat), which is named using the input variable name entered in the interface window. The
 366 generated file can be loaded and executed directly in the MATLAB® workspace using the command
 367 line in MATLAB® and the following command:

```
368 load('outputVariableName.mat');
```

369

370 where “outputVariableName” is the variable name entered in the interface. It is important to
 371 note that in order to successfully load the (*.mat) file into MATLAB® using the above command, the
 372 current folder or MATLAB® path must be set to the folder that contains the (*.mat) file. Once loaded
 373 into the workspace, the variable name will default to “estimatedAbsoluteReflectance”. The user is
 374 also able to import the data structure to MATLAB® using a different initial variable name using the
 375 command:

376

```
377 dataStructure = load('outputVariableName.mat');
```

378

379 where “dataStructure” will be the name of the variable in the MATLAB® workspace. It is
 380 necessary to load the (*.mat) data file with a unique name in the workspace when processing multiple
 381 sets of files and subsequently opening the multiple generated (*.mat) files as each variable will have
 382 an automatic variable name of “estimatedAbsoluteReflectance” in the workspace.

383 The MATLAB® data structure contains 18 fields if all options are enabled in the interface, and
 384 are listed and described in Table 2.

385 **Table 2.** A list and descriptions of the fields in the MATLAB data structure variable.

| Field Name | Description |
|------------|--|
| path | Directory path of the input files |
| name | Name of the input files |
| header | Original ASD header information for the imported files |
| datetime | Date and time information for the imported files |

| | |
|-------------------|--|
| panel | Filename of panel characteristic file |
| latitude | Input latitude value |
| longitude | Input longitude value |
| elevation | Input elevation value |
| reference_zenith | Calculated solar zenith angle for the reference measurement |
| reference_azimuth | Calculated solar azimuth angle for the reference measurement |
| target_zenith | Calculated solar zenith angle for the target measurement |
| target_azimuth | Calculated solar azimuth angle for the target measurement |
| wavelength | An array of type "Double" that contains the wavelength intervals for the imported files |
| reflectance | An array of type "Double" that contains the estimated absolute reflectance values for the imported files |
| IACF | Calculated IACF value for a given file |
| IACF_reflectance | An array of type "Double" that contains the estimated absolute reflectance values with the IACF applied |
| DC_additive | An array of type "Double" that contains the additive solution for the ASD discontinuity correction |
| DC_multiplicative | An array of type "Double" that contains the multiplicative solution for the ASD discontinuity correction |

387 4. User Notes

388 Detailed documentation is provided along with the ASDToolkit download from
389 <http://doi.org/10.5281/zenodo.3996377>. The documents provided include a guide on how to correctly
390 prepare the ASD data files using ViewSpecPro software (to output R_{ratio}), a user guide containing the
391 steps to use the interface as well as details regarding the output files. Images of sample files such as
392 a sample user defined panel characteristic file are included within the user guide to serve as a visual
393 reference for user files. An actual sample panel characteristic file is also included, as it is critical that
394 any user supplied panel characteristic files must match the example formatting.

395 5. Conclusion

396 In situ field or ground reflectance measurements form an important dataset in remote sensing
397 studies, however R_{abs} is not measured directly by field spectrometers and therefore must be
398 calculated. ASDToolkit, a novel MATLAB® processing toolkit, allows for a simple and
399 straightforward batch processing of FieldSpec field spectroscopy data files in order to generate R_{abs}
400 from the R_{ratio} . By creating a linear workflow and using an easy to understand GUI with supporting
401 documentation, users are able to repeatedly process multiple datasets of different sizes collected
402 under various conditions in an efficient manner with traceable results. The files generated by the
403 toolkit are available for further use within MATLAB® and as .csv and are therefore readily converted
404 to different file types dependent upon user requirements.

405

406 **Supplementary Materials:** The following are available online at www.mdpi.com/xxx/s1, Video S1:
407 ASDToolkit_demo_processingSteps.mp4

408 **Author Contributions:** Conceptualization, R.S and J.P.A.M.; methodology, R.S.; software, K.E.; writing—
409 original draft preparation, K.E, R.S. and M.K.; writing—review and editing, K.E., R.S., M.K., J.P.A.M. All authors
410 have read and agreed to the published version of the manuscript.

411 **Funding:** This research was funded by the National Research Council of Canada (NRC) and a Natural Sciences
412 and Engineering Research Council (NSERC) Discovery Frontiers grant that supported the Canadian Airborne
413 Biodiversity Observatory (CABO). The APC was funded by an NSERC Discovery Grant (to Kalacska).

414 **Acknowledgments:** We would like to acknowledge the efforts of Erica Skye Schaaf, who rigorously tested and
415 provided feedback on the ASDToolkit throughout its development. We thank Etienne Laliberté (Université de
416 Montréal) and Nicholas Coops (UBC) for provision of their reference panels through CABO for inclusion in the
417 toolkit.

418 **Conflicts of Interest:** The authors declare no conflict of interest. The funders had no role in the design of the
419 study; in the collection, analyses, or interpretation of data; in the writing of the manuscript, or in the decision to
420 publish the results.

421

422 References

- 423 1. Milton, E. Review article principles of field spectroscopy. *Remote Sensing* **1987**, *8*, 1807-1827.
- 424 2. Milton, E.J.; Schaepman, M.E.; Anderson, K.; Kneubühler, M.; Fox, N. Progress in field spectroscopy.
425 *Remote Sensing of Environment* **2009**, *113*, S92-S109.
- 426 3. Hueni, A.; Damm, A.; Kneubuehler, M.; Schläpfer, D.; Schaepman, M.E. Field and airborne
427 spectroscopy cross validation—Some considerations. *IEEE Journal of Selected Topics in Applied Earth
428 Observations and Remote Sensing* **2016**, *10*, 1117-1135.
- 429 4. Majeke, B.; Van Aardt, J.; Cho, M. Imaging spectroscopy of foliar biochemistry in forestry
430 environments. *Southern Forests: a Journal of Forest Science* **2008**, *70*, 275-285.

- 431 5. Shapira, U.; Herrmann, I.; Karnieli, A.; Bonfil, D.J. Field spectroscopy for weed detection in wheat and
432 chickpea fields. *International journal of remote sensing* **2013**, *34*, 6094-6108.
- 433 6. Choe, E.; van der Meer, F.; van Ruitenbeek, F.; van der Werff, H.; de Smeth, B.; Kim, K.-W. Mapping of
434 heavy metal pollution in stream sediments using combined geochemistry, field spectroscopy, and
435 hyperspectral remote sensing: A case study of the Rodalquilar mining area, SE Spain. *Remote Sensing of*
436 *Environment* **2008**, *112*, 3222-3233.
- 437 7. Peddle, D.R.; White, H.P.; Soffer, R.J.; Miller, J.R.; Ledrew, E.F. Reflectance processing of remote sensing
438 spectroradiometer data. *Computers & geosciences* **2001**, *27*, 203-213.
- 439 8. Gatebe, C.K.; King, M.D. Airborne spectral BRDF of various surface types (ocean, vegetation, snow,
440 desert, wetlands, cloud decks, smoke layers) for remote sensing applications. *Remote Sensing of*
441 *Environment* **2016**, *179*, 131-148.
- 442 9. Soffer, R.J.; Ifimov, G.; Arroyo-Mora, J.P.; Kalacska, M. Validation of Airborne Hyperspectral Imagery
443 from Laboratory Panel Characterization to Image Quality Assessment: Implications for an Arctic
444 Peatland Surrogate Simulation Site. *Canadian Journal of Remote Sensing* **2019**, *45*, 476-508.
- 445 10. Jackson, R.D.; Clarke, T.R.; Moran, M.S. Bidirectional calibration results for 11 Spectralon and 16 BaSO₄
446 reference reflectance panels. *Remote Sensing of Environment* **1992**, *40*, 231-239.
- 447 11. Sandmeier, S.R. Acquisition of bidirectional reflectance factor data with field goniometers. *Remote*
448 *sensing of environment* **2000**, *73*, 257-269.
- 449 12. Georgiev, G.T.; Butler, J.J.; Cooksey, C.; Ding, L.; Thome, K.J. SWIR calibration of spectralon reflectance
450 factor. In Proceedings of Sensors, Systems, and Next-Generation Satellites XV; p. 81760W.
- 451 13. Williams, D.C. Establishment of absolute diffuse reflectance scales using the NPL Reference
452 Reflectometer. *Analytica chimica acta* **1999**, *380*, 165-172.
- 453 14. Bruegge, C.J.; Stiegman, A.E.; Coulter, D.R.; Hale, R.R.; Diner, D.J.; Springsteen, A.W. Reflectance
454 stability analysis of Spectralon diffuse calibration panels. In Proceedings of Calibration of passive
455 remote observing optical and microwave instrumentation; pp. 132-142.
- 456 15. Möller, W.; Nikolaus, K.; Höpe, A. Degradation of the diffuse reflectance of Spectralon under low-level
457 irradiation. *Metrologia* **2003**, *40*, S212.
- 458 16. Stiegman, A.E.; Bruegge, C.J.; Springsteen, A.W. Ultraviolet stability and contamination analysis of
459 Spectralon diffuse reflectance material. *Optical Engineering* **1993**, *32*, 799-805.
- 460 17. Sun, J.; Chu, M.; Wang, M. Degradation nonuniformity in the solar diffuser bidirectional reflectance
461 distribution function. *Applied Optics* **2016**, *55*, 6001-6016.
- 462 18. Rollin, E.; Milton, E.; Emery, D. Reference panel anisotropy and diffuse radiation-some implications for
463 field spectroscopy. *International Journal of Remote Sensing* **2000**, *21*, 2799-2810.
- 464 19. Devices, A.S. FieldSpec 3 User Manual. *ASD Document* **2010**, *600540 Ref. J.*, 92.
- 465 20. Kalacska, M.A.-M., J.P.; Soffer, Ray; Elmer, Kathryn. ASD FieldSpec 3 field measurement protocols.
466 Available online: dx.doi.org/10.17504/protocols.io.qu7dwzn (accessed on
467 [https://www.malvernpanalytical.com/en/support/product-](https://www.malvernpanalytical.com/en/support/product-support/software/ViewSpecProSoftwareInstall.html)
468 [support/software/ViewSpecProSoftwareInstall.html](https://www.malvernpanalytical.com/en/support/product-support/software/ViewSpecProSoftwareInstall.html) (accessed on
469 [https://www.malvernpanalytical.com/en/support/product-](https://www.malvernpanalytical.com/en/support/product-support/software/ViewSpecProSoftwareInstall.html)
470 [support/software/ViewSpecProSoftwareInstall.html](https://www.malvernpanalytical.com/en/support/product-support/software/ViewSpecProSoftwareInstall.html) (accessed on
471 [https://www.malvernpanalytical.com/en/support/product-](https://www.malvernpanalytical.com/en/support/product-support/software/ViewSpecProSoftwareInstall.html)
472 [support/software/ViewSpecProSoftwareInstall.html](https://www.malvernpanalytical.com/en/support/product-support/software/ViewSpecProSoftwareInstall.html) (accessed on
473 [https://www.malvernpanalytical.com/en/support/product-](https://www.malvernpanalytical.com/en/support/product-support/software/ViewSpecProSoftwareInstall.html)
474 [support/software/ViewSpecProSoftwareInstall.html](https://www.malvernpanalytical.com/en/support/product-support/software/ViewSpecProSoftwareInstall.html) (accessed on
- 470 22. Elmer, K. *ASD Raw File Processing Guide*; 2018.
- 471 23. U.S. Naval Observatory, U.K.H.O., H.M. Nautical Almanac Office. *The Astronomical Almanac for the Year*
472 *2015*; U.S. Govt. Printing Office: 2015.
- 473 24. Cornwall, C.; Horiuchi, A.; Lehman, C. NOAA solar position calculator. Available at [http://www.esrl.](http://www.esrl.noaa.gov/gmd/grad/solcalc/azel.html)
474 [noaa.gov/gmd/grad/solcalc/azel.html](http://www.esrl.noaa.gov/gmd/grad/solcalc/azel.html) **2020**.

- 475 25. Hueni, A.; Bialek, A. Cause, effect, and correction of field spectroradiometer interchannel radiometric
476 steps. *IEEE Journal of Selected Topics in Applied Earth Observations and Remote Sensing* **2017**, *10*, 1542-1551.
- 477 26. Hemmer, T.H.; Westphal, T.L. Lessons learned in the postprocessing of field spectroradiometric data
478 covering the 0.4-2.5-um wavelength region. In *Proceedings of Algorithms for Multispectral,
479 Hyperspectral, and Ultraspectral Imagery VI*; pp. 249-260.
- 480 27. Mac Arthur, A.; MacLellan, C.J.; Malthus, T. The fields of view and directional response functions of
481 two field spectroradiometers. *IEEE transactions on geoscience and remote sensing* **2012**, *50*, 3892-3907.
- 482 28. Karami, M. *asd_jumpcorrection*, MATLAB Central File Exchange, 2012.
- 483 29. Robinson, I. *Field Spectroscopy Facility Post Processing Toolbox*, 1.3.1; MATLAB Central File Exchange,
484 2011.
- 485